Gastroenterology 2026;171:50–65

GI CANCER

STING Ablation in T Cells Is Required for the Efficacy of STING Agonists in CAR-T Cell Immunotherapy of Pancreatic Cancer

Ignazio Piseddu,[1,2,3] Rebekka Endres,[1,2] Fabian Lanzl,[1,2] Linda Hammann,[2,3] Marleen Bérouti,[1] Matthias Thaler,[3,4] Lisa Fahr,[2] Hannah Fischer,[1] Varvara Varlamova,[1] Jan Gärtig,[3] Daniel Nixdorf,[5,6] Patrick Layritz,[3] Charlotte Marx,[3] Christine Hörth,[3] Catharina Witte,[2,3] Alpay Bulut,[1,2] David Illig,[7] Anne Marie Senz,[3] Lesca Holdt,[8] Ivonne Regel,[2] Adrian Gottschlich,[3,6,9] Marion Subklewe,[5,6] Julia Mayerle,[2,9] David Anz,[2,3] Sebastian Kobold,[3,9,10,11] **Andreas Linder,**[1,2,§] and **Veit Hornung**[1,12,§]

[1]Gene Center and Department of Biochemistry, Ludwig-Maximilians-Universität München, Munich, Germany; [2]Department of Medicine II, LMU University Hospital, Ludwig-Maximilians-Universität München, Munich, Germany; [3]Institute of Clinical Pharmacology, LMU University Hospital, Ludwig-Maximilians-Universität München, Munich, Germany; [4]Medizinische Klinik und Poliklinik IV, Division of Rheumatology and Clinical Immunology, LMU University Hospital, Ludwig-Maximilians-Universität München, Munich, Germany; [5]Laboratory for Translational Cancer Immunology, LMU Gene Center, Munich, Germany; [6]Department of Medicine III, LMU University Hospital, Ludwig-Maximilians-Universität München, Munich, Germany; [7]Department of Pediatrics, Dr. von Hauner Children's Hospital, LMU University Hospital, Ludwig-Maximilians-Universität München, Munich, Germany; [8]Institute of Laboratory Medicine, LMU University Hospital, Ludwig-Maximilians-Universität München, Munich, Germany; [9]German Cancer Consortium (DKTK), Partner Site Munich, a partnership between the DKFZ Heidelberg and the University Hospital of the LMU, Munich, Germany; [10]Einheit für Klinische Pharmakologie (EKLiP), Helmholtz Zentrum München - German Research Center for Environmental Health, Neuherberg, Germany; [11]German Center for Lung Research (DZL), Partner Site Munich, Munich, Germany; and [12]Cluster for Nucleic Acid Sciences and Technologies – NUCLEATE, Munich, Germany

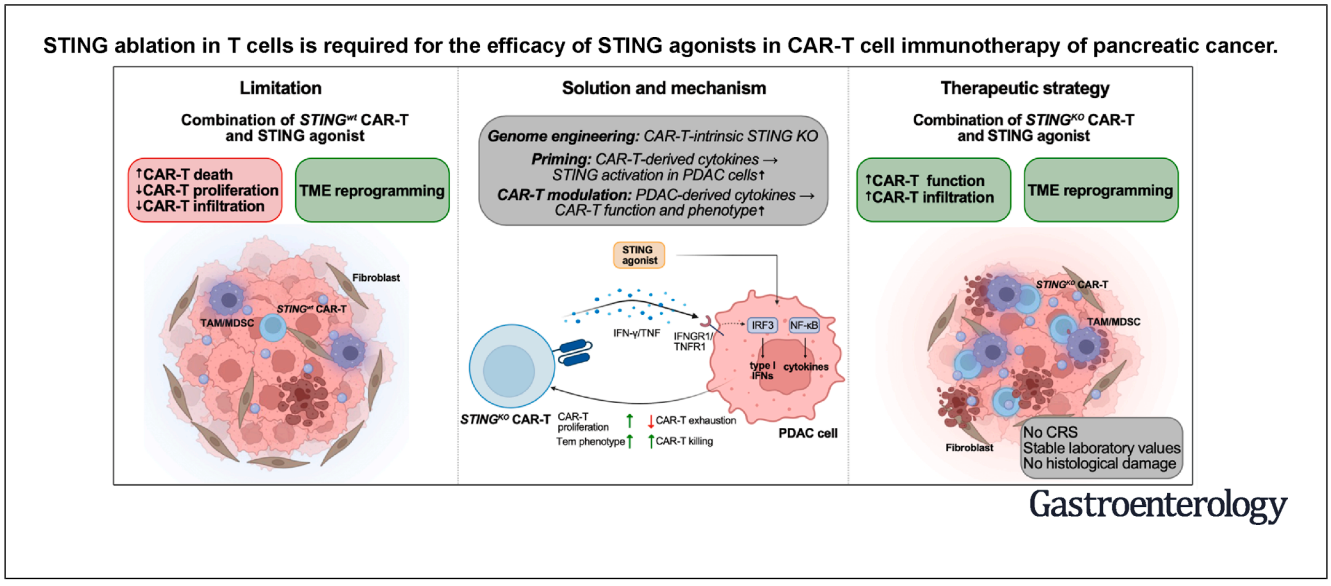

BACKGROUND & AIMS: Chimeric antigen receptor (CAR) T cells have shown great potential in hematological cancers, but lack efficacy in solid tumors, highlighting the need for novel strategies. Stimulator of interferon genes (STING) activation was shown to inflame the tumor microenvironment, but combination of STING agonists and CAR-T cells might be limited by detrimental outcomes of T cell–intrinsic STING activation. In this study, we evaluated the potential of combining STING agonists and CAR-T cells in the context of pancreatic cancer. **METHODS:** We assessed the synergy of CRISPR-Cas9–edited CAR-T cells and the STING agonist diABZI within a T cell exhaustion model in vitro and both xenograft and syngeneic mouse models in vivo. **RESULTS:** Combination of STING-ablated CAR-T cells and diABZI resulted in enhanced cancer cell killing, increased CAR-T cell proliferation, reduced exhaustion, and expansion of an effector-memory phenotype in vitro. Mechanistically, superior CAR-T cell functionality required genetic ablation of *STING* in CAR-T cells and was dependent on cancer cell–intrinsic STING signaling on STING-agonistic treatment. Moreover, we identified a synergistic feedback loop comprising the T cell–secreted cytokines interferon-γ and tumor necrosis factor, which prime STING signaling within cancer cells, thereby potentiating the outcomes of cancer cell–intrinsic STING activation in inducing

ameliorated CAR-T cell states. Ultimately, we could demonstrate that combination of *STING* deficient CAR-T cells and diABZI was able to provide enhanced tumor control in both xenograft and syngeneic mouse models. This was accompanied by increased intratumoral CAR-T cell numbers and reprogramming of the tumor microenvironment in vivo. **CONCLUSIONS:** Our findings suggest that *STING* deficient CAR-T cells stand to benefit from STING agonists to improve CAR-T cell therapy for immune-deprived cancers such as pancreatic cancer.

Keywords: CAR-T Cells; STING; CRISPR-Cas9; PDAC.

Pancreatic ductal adenocarcinoma (PDAC) represents one of the most lethal cancers, with a 5-year survival rate of around 12%.[1] Despite significant advancements in targeted therapies and immunotherapies for other types of solid cancers, PDAC continues to exhibit a poor response to both conventional as well as immunotherapeutic approaches.[2] This resistance is largely attributed to its aggressive nature and "immune-cold" tumor microenvironment (TME), characterized by low T cell infiltration and dominant immunosuppression.[2] Thus, novel treatment strategies are urgently needed to improve therapeutic outcomes and patient survival.

Chimeric antigen receptor (CAR) T cells represent a novel immunotherapeutic approach that has revolutionized the treatment of hematological malignancies[3]; however, this remarkable success has yet to be realized in the context of solid tumors, including PDAC.[4] The main limitations of CAR-T cell therapy in solid cancer entities comprise limited infiltration, low persistence, and intratumoral T cell dysfunction.[3,4] Therefore, strategies to overcome these barriers are required to extend CAR-T cell efficacy to non-hematological cancers.

Targeting tumor-intrinsic pathways and the TME are possible strategies to overcome these limitations and are under active preclinical and clinical investigation.[5] In this context, the cyclic GMP-AMP synthase (cGAS)-stimulator of interferon genes (STING) pathway, a cytosolic DNA sensor central to innate immunity, has emerged as a key driver of antitumor immune responses.[6,7] Activation of this pathway has been described to promote cancer cell death, antigen release, dendritic cell–mediated antigen presentation and T cell priming, as well as to facilitate T cell trafficking into tumors, thereby potentiating anticancer immunity.[7] In PDAC, treatment with STING agonists has been shown to effectively alter tumor architecture and immune profile, thereby reversing PDAC immune privilege and prolonging survival in preclinical models.[8–10] Therefore, leveraging intratumoral STING activation in PDAC might represent a promising strategy to overcome major limitations of CAR-T cell therapy in this entity.

However, although the functionality of the cGAS-STING axis has been traditionally assigned to innate immune cells and cancer cells, recent evidence has demonstrated that this pathway is preserved, but has detrimental effects in T cells. STING agonists have been shown to promote T cell senescence and apoptosis by activating T cell–intrinsic STING signaling, which limits their effects as antitumor regimens.[11,12] Thus, a combination of STING agonists and therapeutic T cells might require the protection of CAR-T cells from detrimental outcomes of T cell–intrinsic STING activation. Technological advances in genetic engineering of

WHAT YOU NEED TO KNOW

BACKGROUND AND CONTEXT

CAR-T cells have shown great potential in hematological cancers, but lack efficacy in solid tumors, including pancreatic cancer.

NEW FINDINGS

In this study, we demonstrate that combination of CRISPR-Cas9–edited, STING–ablated CAR-T cells and synthetic STING agonists results in enhanced CAR-T cell functionality in vitro and increased tumor control, enhanced intratumoral CAR-T cell infiltration, and reprogramming of the tumor microenvironment in vivo.

LIMITATIONS

These investigations were performed in mice. Thus, clinical trials in humans investigating safety and efficacy of this approach in a human context are required.

CLINICAL RESEARCH RELEVANCE

Our data propose that the combination of *STING*^{KO} CAR-T cells and STING agonists represents a safe and powerful strategy to enhance CAR-T cell functionality and to overcome major limitations of adoptive T cell therapy in the context of poorly immunogenic solid tumors such as pancreatic cancer, thus holding promise to represent a major progress in the field of CAR-T cell therapy in solid cancers.

BASIC RESEARCH RELEVANCE

These data suggest that the combination of CRISPR-Cas9–edited therapeutic T cells with agonists of the cGAS-STING pathway is a promising strategy to increase intratumoral CAR-T cell infiltration, reduce CAR-T cell exhaustion, and to modify CAR-T cell proliferation and phenotype. Furthermore, this study provides mechanistic insights into a potent synergistic feedback loop, initiated by T cell–secreted cytokines, which sensitize cancer cells to therapeutic STING activation, thus potentiating beneficial effects on the therapeutic T cell product.

§ **Authors share co-senior authorship.**

Abbreviations used in this paper: **CAR, chimeric antigen receptor; cGAS, cyclic GMP-AMP synthase; hMSLN, human mesothelin; IFN, interferon; IFNGR1, interferon-gamma receptor 1; IL, interleukin; IP-10, interferon-gamma inducible protein 10; IRF3, interferon regulatory factor 3; IV, intravenous; KO, knockout; LDH, lactate dehydrogenase; MDSC, myeloid-derived suppressor cell; PDAC, pancreatic ductal adenocarcinoma; SC, subcutaneous; STING, stimulator of interferon genes; TAM, tumor-associated macrophage; TME, tumor microenvironment; TNFR1, tumor necrosis factor receptor 1; WT, wild type.**

Most current article

0016-5085
https://doi.org/10.1053/j.gastro.2026.01.031

primary human T cells holds the promise to engineer cells with high precision and low off-target effects also for clinical application. Thus, genetic modification of detrimental T cell–intrinsic pathways is a promising approach to enhance T cell–mediated anticancer responses and to facilitate the use of combination agents to overcome limitations of CAR-T cell therapy in solid tumors.

In this study, we sought to evaluate the efficacy of CAR-T cell therapy in combination with STING agonism in human and murine preclinical models of PDAC. In light of previous reports on the detrimental effects of STING activation in T cells, we focused on the role of T cell–intrinsic STING engagement and its impact on cellular immunotherapy.

Methods

Cell Lines

All human and murine cell lines used and their respective cell culture requirements are provided in the Supplementary Methods section.

Isolation and Culture of Human T Cells

Peripheral blood mononuclear cells were isolated, resuspended in MACS buffer, and human pan T cells were negatively selected using magnetic bead isolation. Isolated T cells were rested overnight in human resting T cell medium before performing CRISPR-Cas9 knockouts (see the next section). After CRISPR knockout, T cells were activated using CD3/CD28 Dynabeads (Thermo Fisher) in human activating T cell medium and expanded every 2 to 3 days.

CRISPR-Cas9 Knockout Generation

Polyclonal CRISPR-Cas9 T cell knockouts were generated as described previously.[12,13] Briefly, RNPs were produced by mixing synthesized, chemically stabilized trans-activating CRISPR RNA (tracrRNA) and CRISPR RNA (crRNA) (both IDT; 100 pmol each), annealing them at 95°C for 5 minutes, then letting them cool at room temperature for 30 minutes. tracr:crRNA pairs were then incubated with 40 pmol of recombinant S.p. NLS-Cas9 (IDT) for at least 15 minutes at room temperature. A detailed description of knockout generation and guide RNA sequences are provided in the Supplementary Methods section.

CAR-T Cell Generation

The human CAR construct used was a second-generation CAR vector system containing CD28 and CD3ζ signaling domains, as previously described.[14,15] Human T cell transduction has been performed as previously published.[14] Murine anti-EpCAM-mCherry CAR-T cells were generated as described previously.[15] A detailed protocol of human and murine CAR-T cell generation is provided in the Supplementary Methods.

Animal Experiments

Six- to 10-week-old female C57BL/6J or NSG mice (NOD.Cg-Prkdcscid Il2rgtm1WjI/SzJ) were purchased from Janvier. The ARRIVE (Animal Research: Reporting of In Vivo Experiments) guidelines were applied. The SUIT-2 xenograft model was established by subcutaneous (SC) injection of 10^6 cells into the flank, followed by intravenous (IV) injection of 10^7 CAR-T cells. For combination treatment, 1.5 mg/kg diABZI (Selleck Chemicals) or vehicle control was injected intratumorally. The syngeneic SC and orthotopic T11-EpCAM models were generated similarly, with 0.75 mg/kg diABZI or 1 mg/kg diABZI, respectively, vs vehicle IV and 10^7 EpCAM-CAR-T cells derived from wild-type (WT) or *Sting1*$^{-/-}$ mice. For safety assessment, serum cytokine concentrations were analyzed using the LEGENDplex MU Cytokine Release Syndrome Panel (13-plex) kit (Biolegend) according to the manufacturer's protocol and kidney and liver function parameters were determined by the Institute of Laboratory Medicine (LMU University Hospital) according to standard procedures. All experiments were approved by local authorities.

In Vitro CAR-T Cell Killing Assays

A total of 3×10^4 human mesothelin (hMSLN)-SUIT-2 cells were plated 1 day before T cell coincubation in a 96-well flat-bottom plate in Dulbecco's modified Eagle's medium. The next day, medium was removed from tumor cells and CAR-T cells were added in an effector-to-target ratio of 1:5 in human T cell medium without cytokines. In addition, control medium or medium containing 0.1 μM diABZI was added to the coculture. After 24 hours, 48 hours, and 72 hours, supernatants were harvested and lactate dehydrogenase (LDH) release was analyzed using CyQuant LDH cytotoxicity assay (Invitrogen), according to the manufacturer's instructions. Relative LDH release was calculated as *LDH release [%] = 100 × (measurement − medium control)/(lysis control − medium control).*

Repetitive Antigen Stimulation Assay

A total of 0.2×10^6 hMSLN-SUIT-2 cells were plated 1 day before the experiment. On day 0, tumor cells received 0.2×10^6 hMSLN-specific CAR-T cells and 0.1 μM diABZI (or 10 μM SNX281; MedChemExpress) or control medium. Every 2 days, supernatants containing CAR-T cells were transferred to freshly plated tumor cells, with 200 to 300 μL fresh RPMI added. On day 7, T cells were centrifuged, resuspended in fresh medium with diABZI or control, and replated. The transfer process continued every 2 days. On day 14, CAR-T cells were counted and analyzed via a 72-hour killing assay with adjusted cell numbers in an effector-to-target ratio of 1:5 to assess per-cell cytotoxic function without further diABZI addition and flow cytometry.

Antibodies and Flow Cytometry

Flow cytometry–based immunophenotyping was performed by washing the cells of interest once with phosphate-buffered saline, followed by subsequent staining for 30 minutes at 4°C with 1:500 Zombie Aqua Fixable Viability Dye (Invitrogen) and 1:100 to 1:200 dilutions of the respective staining antibodies. Subsequently, cells were analyzed on a BD LSRFortessa (BD Biosciences). Data were analyzed using FlowJo software (BD Biosciences).

Immunohistochemistry

Immunohistochemical staining was performed on 3-μm sections of formalin-fixed, paraffin-embedded tissue from 11 chemotherapy-naïve patients with PDAC. After deparaffinization, rehydration, and antigen retrieval in sodium citrate (pH 6), sections were blocked and incubated overnight at 4°C with

STING antibody (1:100) (D2P2F rabbit immunoglobulin G, #13647, Cell Signaling Technology). Secondary antibody incubation followed for 2 hours at room temperature before 3,3'-Diaminobenzidine (DAB) staining, hematoxylin counterstaining, and mounting. Whole-slide scans were generated using a Pannoramic MIDI II scanner. STING immunohistochemical staining was quantified with QuPath (0.5.1)[16] using a trained object classifier to distinguish stroma, immune, and tumor cells based on morphological criteria, with STING-positive cells quantified as a percentage of detected cells. Hematoxylin-eosin staining was performed according to standard protocols.

Data Visualization and Statistical Analysis

Data were visualized using GraphPad Prism version 10 (GraphPad Software Inc) and Affinity Designer (Serif). All data are presented as means and error bars show SEM. Statistical analyses were performed using Prism 10. Illustrations and treatment schemes were generated using biorender.com.

More details on the methods used in this article are provided in the Supplementary Methods.

Results

Combination of STING Agonists and STING^{KO} CAR-T Cells Results in Enhanced Killing Capacity on Repetitive Antigen Stimulation In Vitro

To investigate the role of STING in T cells within the context of immunotherapy using STING agonists, we focused on PDAC, a solid tumor resistant to standard immunotherapy. As previously reported,[17] we found STING highly expressed in primary human PDAC tissues from chemotherapy-naïve patients via immunohistochemistry (Figure 1*A*). STING was present in cancer cells, stroma, and immune cells, with the highest expression in cancer cells, followed by immune and stroma cells (Figure 1*A*, right), suggesting these populations as targets for STING agonists in PDAC. To assess the combination of STING-deficient CAR-T cells and STING agonists in an antigen-dependent setting, we used CAR-T cells targeting hMSLN and SUIT-2 cells transgenic for this antigen (Supplementary Figure 1*A* and *B*), a model resistant to nonengineered CAR-T cells in vivo.[14,15] The non-nucleotide STING agonist diABZI was used for its superior pharmacodynamics over cyclic-dinucleotide–based ligands.[18] Using RNPs, we targeted *STING1* (encoding STING) in primary human T cells, completely abolishing STING protein expression (Figure 1*B*). CAR transduction efficiencies were similar in WT and *STING* knockout (*STING*^{KO}) T cells (Supplementary Figure 1*C*). Given that STING activation induces apoptosis in T cells, we examined diABZI-mediated apoptosis upon tumor cell encounter (Supplementary Figure 1*D* and *E*). diABZI treatment increased T cell death in *STING*^{wt} CAR-T cells, consistent with prior findings, whereas *STING*^{KO} CAR-T cells were protected from apoptosis (Supplementary Figure 1*D*).

To compare cytotoxicity of *STING*^{KO} CAR-T cells and WT controls against SUIT-2 cells, we conducted killing assays over 72 hours. Baseline killing capacity was comparable between WT and *STING*^{KO} CAR-T cells (Supplementary Figure 1*F*, left). In the presence of diABZI, *STING*^{KO} CAR-T cells exhibited slightly increased killing, whereas *STING*^{wt} CAR-T cells showed a moderate reduction in killing (Supplementary Figure 1*F*, right). Interferon (IFN)-γ secretion followed a similar pattern (Supplementary Figure 1*G*). To better mimic complex in vivo interactions, we used a 14-day "exhaustion" model in which CAR-T cells repeatedly encountered their cognate antigen with or without STING agonism (Figure 1*C*). After this period, both *STING*^{wt} and *STING*^{KO} CAR-T cells lost their killing capacity when rechallenged with fresh tumor cells in the absence of diABZI (Figure 1*D*, left). In contrast, *STING*^{KO} CAR-T cells retained robust cytotoxicity and IFN-γ secretion when combined with diABZI, whereas *STING*^{wt} CAR-T cells remained dysfunctional (Figure 1*D*, right, and Figure 1*E*). No benefit from diABZI was observed with untransduced T cells, confirming antigen specificity (Supplementary Figure 1*H*). We observed similar effects regarding cytotoxicity (Figure 1*F*) and IFN-γ secretion (Supplementary Figure 1*I*) using SNX281, an alternative small molecule STING agonist.

In summary, these results suggest that combining a STING agonist with STING-deficient CAR-T cells enhances CAR-T cell killing capacity and IFN-γ secretion under T cell exhaustion conditions in vitro.

STING^{KO} CAR-T Cells Combined With diABZI Show Enhanced CAR-T Cell Functionality

Having observed that diABZI enhanced *STING*^{KO} CAR-T cell functionality, we aimed to characterize its effects on CAR-T cells by assessing absolute numbers and phenotypes of CAR-T cells at day 14 of repetitive antigen stimulation. For comparability, CAR-T cell expansion data were normalized to *STING*^{wt} CAR-T cells without diABZI. We observed a dramatic reduction in cell numbers (Figure 2*A*) and viability (Supplementary Figure 2*A*) when *STING*^{wt} CAR-T cells were treated with diABZI, consistent with its pro-apoptotic effects. In contrast, *STING*^{KO} CAR-T cells exposed to diABZI showed a 30-fold increase in cell numbers (Figure 2*A*). Consistently, CAR-T frequencies dropped in all groups 24 hours after tumor cell encounter, except for *STING*^{KO} CAR-T plus diABZI, where frequencies remained substantially high (Supplementary Figure 2*B*), suggesting enhanced persistence and potential resistance to activation-induced cell death. Exhaustion markers TIM-3 and LAG-3 were initially low in all groups but increased over time, remaining moderate in *STING*^{KO} CAR-T cells with diABZI (Figure 2*B*), with similar patterns for PD-1/LAG-3 and PD-1/TIM-3 coexpression (Supplementary Figure 2*C*). T cell activation markers CD44/CD107a moderately increased in both diABZI-treated groups, regardless of genotype (Supplementary Figure 2*D*). Assessing CD45RA and CCR7 expression revealed decreased effector-like (Teff) T cells in *STING*^{KO} CAR-T cells with diABZI, whereas effector-memory-like (Tem) cells expanded compared with the other conditions (Figure 2*C* and *D*). To validate our findings in a different cell line, we used

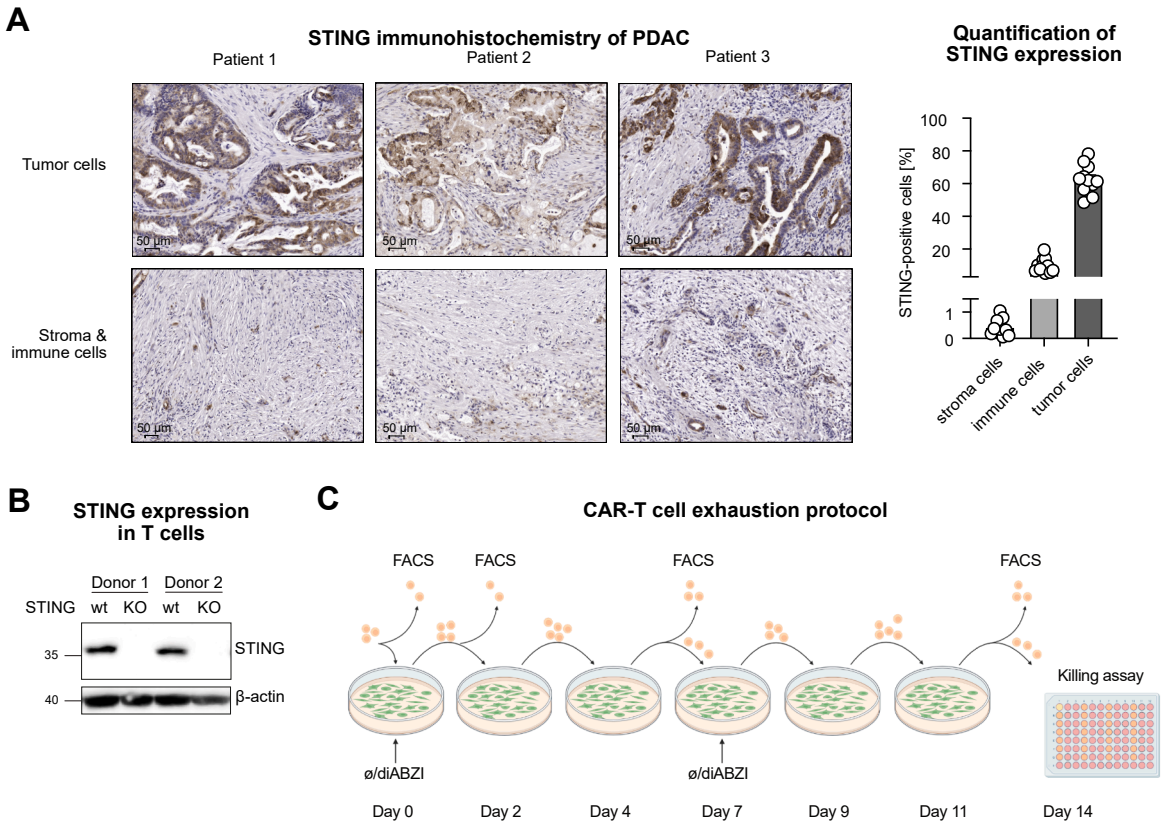
A
STING immunohistochemistry of PDAC
Patient 1
Patient 2
Patient 3
Tumor cells
Stroma & immune cells
50 µm
Quantification of STING expression
STING-positive cells [%]
100
80
60
40
20
1
0
stroma cells
immune cells
tumor cells
B
STING expression in T cells
Donor 1
Donor 2
STING wt KO wt KO
35
40
STING
β-actin
C
CAR-T cell exhaustion protocol
FACS
FACS
FACS
FACS
Killing assay
ø/diABZI
ø/diABZI
Day 0
Day 2
Day 4
Day 7
Day 9
Day 11
Day 14
D
SUIT-2 cell lysis
P < .0001
P < .0001
P < .0001
P < .0001
P < .0001
P < .0001
cell killing [%]
80
60
40
20
0
time [h]
24 48 72 24 48 72 24 48 72 24 48 72
ø
+ diABZI
STINGwt CART
STINGKO CART
E
IFN-γ secretion
P = 0140
P = 0124
P = 0138
IFNγ [pg/ml]
1500
1000
500
0
ø
+ diABZI
STINGwt CART
STINGKO CART
F
SUIT-2 cell lysis 72h - SNX281
P = .0009
P = .0011
P < .0001
P > .9999
P < .0001
cell killing [%]
80
60
40
20
0
ø
+ diABZI
+ SNX281
STINGwt CART
STINGKO CART

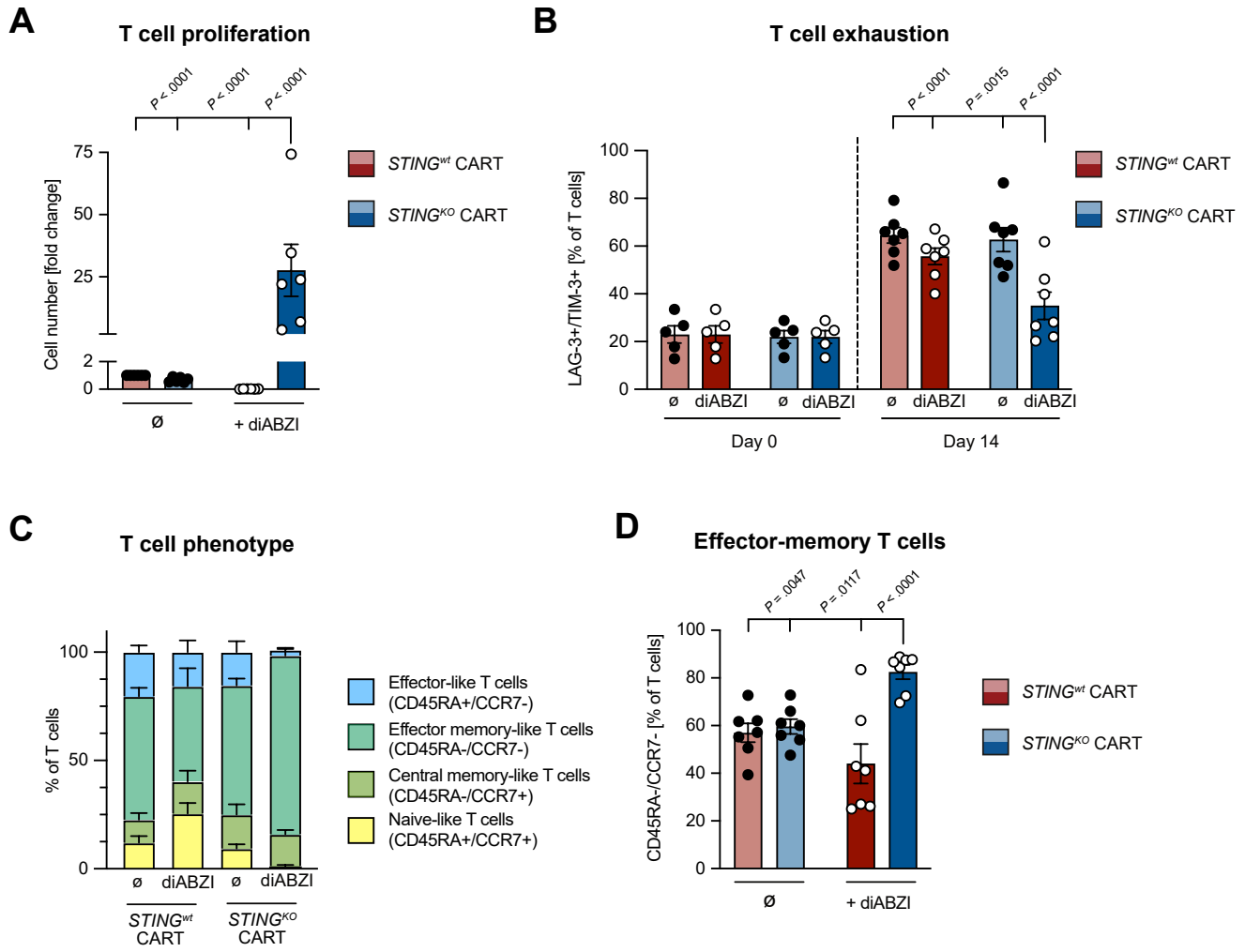

Figure 2. *STING*^{KO} CAR-T cells combined with diABZI show enhanced CAR-T cell functionality. (*A–D*) At day 14 of repetitive antigen stimulation, CAR-T cells were analyzed by flow cytometry. Statistical analysis was performed using 2-way analysis of variance with Sidak's multiple comparisons test. (*A*) Absolute CAR-T counts were determined. Fold changes were determined relative to *STING*^{wt} CAR-T + ø. Graph shows mean ± SEM of 6 independent donors. Statistical analysis was conducted on log-transformed data. (*B*) LAG-3/TIM-3 coexpression was determined at day 0 and day 14. Graph shows mean ± SEM of 5 (day 0) and 7 (day 14) independent donors. (*C*) CD45RA and CCR7 expression were determined. Graph shows mean ± SEM of 7 independent donors. (*D*) Frequencies of effector-memory T cells (CD45RA-/CCR7-) were analyzed. Graph shows mean ± SEM of 7 independent donors.

AsPC-1 cells, a PDAC line endogenously expressing hMSLN.[19] Similar effects were observed regarding cytotoxicity (Supplementary Figure 2*E*), proliferation (Supplementary Figure 2*F*, left), exhaustion (Supplementary Figure 2*F*, right), and Tem phenotype formation in *STING*^{KO} CAR-T cells plus diABZI (Supplementary Figure 2*G* and *H*), consistent with SUIT-2 results.

Taken together, *STING*^{KO} CAR-T cells combined with diABZI exhibited improved proliferation, reduced exhaustion, and expanded Tem phenotype.

Figure 1. Combination of STING agonists and *STING*^{KO} CAR-T cells results in enhanced killing capacity upon repetitive antigen stimulation in vitro. (*A*) Representative immunohistochemistry of STING in 3 of 11 PDAC tissues. Data from 11 individual samples are depicted as mean values ± SEM. (*B*) STING protein expression in unedited and *STING*^{KO} T cells. β-Actin was used as loading control. One representative immunoblot of 3 independent experiments is depicted. (*C*) Schematic illustration of T cell exhaustion protocol. (*D*) Cell lysis was determined using LDH release assay. Graph shows mean ± SEM of 10 independent donors. Statistical analysis was conducted by 2-way analysis of variance (ANOVA) with Tukey's multiple comparisons test. (*E*) IFN-γ in supernatants at day 3 of the final killing experiment was determined using enzyme-linked immunosorbent assay. Data show mean ± SEM of 6 independent donors. Statistical analysis was conducted using 2-way ANOVA with Sidak's multiple comparisons test. (*F*) T cell exhaustion protocol was performed using SNX281 instead of diABZI. Cell lysis was determined using LDH release assay. Graph shows mean ± SEM of 6 independent donors. Statistical analysis was conducted by 2-way ANOVA with Sidak's multiple comparisons test.

Tumor Cell–Intrinsic STING Signaling Is Required for Enhanced Functionality of STING^{KO} CAR-T Cells

The observation that diABZI enhanced *STING*^{KO} CAR-T cell functionality suggested a requirement for tumor cell–intrinsic STING signaling. To investigate this, we generated STING-deficient SUIT-2 cells (Figure 3*A*) and repeated the CAR-T cell exhaustion protocol on *STING*^{KO} tumor cells, followed by a killing experiment on *STING*^{wt} cancer cells (Supplementary Figure 3*A*). In this setting, *STING*^{KO} CAR-T cells combined with diABZI were as dysfunctional as other conditions in cancer cell killing and IFN-γ secretion (Figure 3*B* and *C*). CAR-T cell numbers remained unchanged in *STING*^{KO} CAR-T cells with diABZI compared with untreated controls (Figure 3*D*). In addition, coexpression of LAG-3/TIM-3 was strongly increased in *STING*^{KO} CAR-T cells with diABZI, similar to other conditions (Figure 3*E*). This pattern was also observed for PD-1/LAG-3 (Supplementary Figure 3*B*, left) and PD-1/TIM-3 (Supplementary Figure 3*B*, right). Coexpression of activation markers CD44/CD107a was comparable across all groups, with no evidence of enhanced activation in diABZI-treated groups (Supplementary Figure 3*C*). Effector-memory phenotype formation was unaltered in *STING*^{KO} CAR-T cells with diABZI relative to other conditions (Figure 3*F*).

Altogether, these findings indicate that intact tumor cell–intrinsic STING signaling is required to mediate superior CAR-T cell functionality in the combination of *STING*^{KO} CAR-T cells and diABZI.

Tumor-Intrinsic IRF3 and NF-κB Support STING^{KO} CAR-T Cell Proliferation Upon STING Agonist Treatment

Because tumor cell–intrinsic STING signaling was required for superior CAR-T cell functionality, we sought to identify the downstream pathways involved. On activation, STING translocates to the Golgi, activating TBK1 and interferon regulatory factor 3 (IRF3), and inducing nuclear factor (NF)-κB signaling[20] (Figure 4*A*). To determine whether both pathways were engaged, we measured IFN-β and interferon-gamma inducible protein 10 (IP-10) as IRF3 proxies (Figure 4*B*) and interleukin (IL)-6 as a NF-κB target in cocultures of *STING*^{KO} CAR-T cells with WT or *STING*^{KO} SUIT-2 cells (Figure 4*C*). IFN-β, IP-10, and IL-6 levels were increased in diABZI-treated cocultures with STING-expressing cancer cells, but not with *STING*^{KO} SUIT-2. To assess the contributions of IRF3 and NF-κB to superior *STING*^{KO} CAR-T cell functionality, we generated hMSLN-SUIT-2 cells deficient for *IRF3*, *IFNAR1*, and the NF-κB component *RELA* (Supplementary Figure 4*A*). Using 2 independent KO clones per genotype, we conducted the T cell exhaustion assay followed by a killing experiment with *STING*^{KO} CAR-T cells on WT SUIT-2 (Supplementary Figure 4*B*). Proliferation of *STING*^{KO} CAR-T cells with diABZI was reduced when cocultured with *IRF3*- or *RELA*-deficient cancer cells (Figure 4*D* and *E*) with a more pronounced effect on *RELA* deletion. *IFNAR1* deletion had minimal impact (Supplementary Figure 4*C*). Next, we evaluated *STING*^{KO} CAR-T cell killing capacity in the presence of *IRF3*, *IFNAR1*, or *RELA* deletion (Figure 4*F* and *G*; Supplementary Figure 4*D*). *STING*^{KO} CAR-T cells incubated with WT hMSLN-SUIT-2 served as a positive control. *IRF3* (Figure 4*F*) and *IFNAR1* deletion (Supplementary Figure 4*D*) had no effect, whereas *RELA* deletion moderately reduced cytotoxicity (Figure 4*G*). Exhaustion marker expression remained elevated when cocultured with *IRF3*- or *RELA*-deficient, but not *IFNAR1*-deficient SUIT-2, although the differences were not statistically significant (Supplementary Figure 4*E*–*G*).

Overall, these data indicate that therapeutic STING agonism requires both IRF3 and NF-κB activation in cancer cells to enhance *STING*^{KO} CAR-T cell proliferation.

Priming of Target Cell–Intrinsic STING Activation by IFN-γ and TNF Is Crucial for Enhanced STING^{KO} CAR-T Cell Fitness

Upon antigen encounter, CAR-T cells secrete effector cytokines, particularly IFN-γ and tumor necrosis factor (TNF).[21] Because both cytokines regulate the activation threshold of the STING pathway,[22,23] we examined their role in enhancing CAR-T cell functionality. To assess their contribution, we analyzed STING phosphorylation in hMSLN-SUIT-2 cells (Figure 5*A*). Prestimulation with IFN-γ, TNF, or both increased pSTING band intensity, suggesting enhanced STING phosphorylation upon diABZI stimulation. Consequently, we observed higher IP-10 secretion (Figure 5*B*) as well as enhanced cell death induction on diABZI stimulation in IFN-γ/TNF-pretreated cancer cells (Figure 5*C*). To determine whether cytokine priming was necessary for enhanced *STING*^{KO} CAR-T cell functionality with diABZI, we generated *IFNGR1*$^{-/-}$, *TNFR1*$^{-/-}$, and double-deficient hMSLN-SUIT-2 cells (Supplementary Figure 5*A*). Using 2 independent KO clones per genotype, we performed the T cell exhaustion assay followed by a killing experiment in WT SUIT-2 cells (Supplementary Figure 5*B*). As already observed, *STING*^{KO} CAR-T cells combined with diABZI on WT SUIT-2 exhibited increased cell numbers compared with *STING*^{wt} CAR-T cells without diABZI (Figure 5*D*). *TNFR1* deletion slightly weakened this effect, whereas *IFNGR1* deletion, alone or with *TNFR1*, resulted in near-complete loss of proliferation, indicating a crucial role for interferon-gamma receptor 1 (IFNGR1) signaling. In addition, exhaustion marker reduction seen with *STING*^{KO} CAR-T cells and diABZI was abolished on IFNGR1 or tumor necrosis factor receptor 1 (TNFR1)/IFNGR1 deletion (Supplementary Figure 5*C*). Next, we evaluated CAR-T cell killing capacity under *IFNGR1* and *TNFR1* deletion. *STING*^{KO} CAR-T cells incubated with unmodified hMSLN-SUIT-2 served as a positive control, whereas unmodified CAR-T cells expanded on these cells were a negative control. *TNFR1* or *IFNGR1* deletion reduced *STING*^{KO} CAR-T cell killing capacity, whereas dual receptor deletion resulted in complete dysfunctionality,

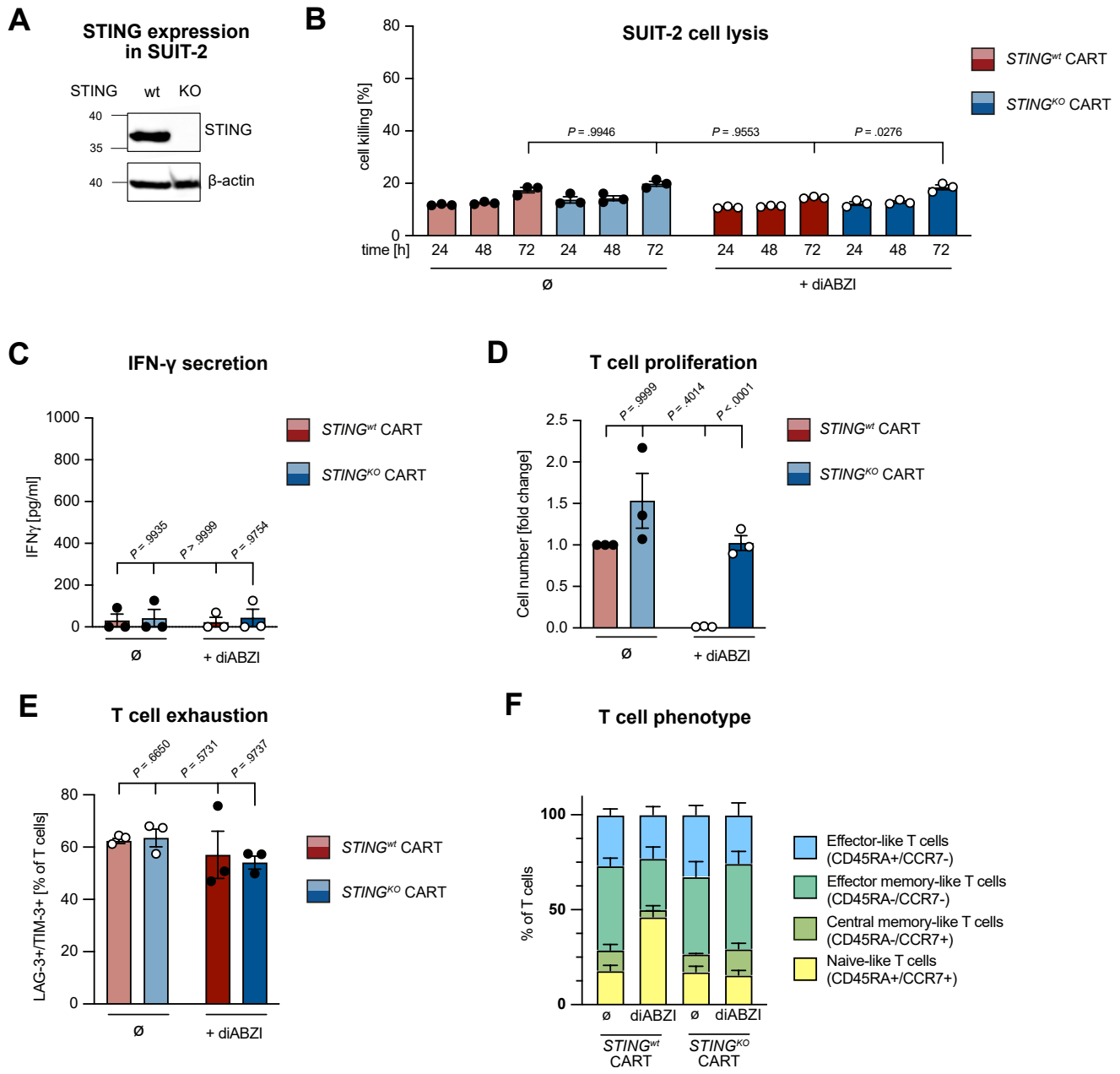

Figure 3. Tumor cell–intrinsic STING signaling is required for enhanced functionality of *STING*^{KO} CAR-T cells. (*A*) Immunoblot of STING in unedited and *STING*^{KO} hMSLN-SUIT-2 cells. β-Actin was used as loading control. One representative immunoblot of 3 independent experiments is depicted. (*B–F*) At day 14 of repetitive antigen stimulation, 6×10^3 CAR-T cells were co-incubated with 3×10^4 hMSLN-SUIT-2 cells. Graphs show mean ± SEM of 3 independent donors. Statistical analysis was performed using 2-way analysis of variance with Tukey's multiple comparisons test. (*B*) Cancer cell lysis was determined using LDH release assay. (*C*) IFN-γ expression in supernatants was determined using enzyme-linked immunosorbent assay. (*D*) Absolute CAR-T counts were determined by flow cytometry. Fold changes were determined relative to *STING*^{wt} CAR-T cells + ø. Statistical analysis was conducted on log-transformed data. (*E*) LAG-3/TIM-3 coexpression was determined using flow cytometry. (*F*) CD45RA and CCR7 expression were determined via flow cytometry.

similar to *STING*^{wt} CAR-T cells without combination treatment (Figure 5*E*).

Taken together, these findings suggest that cancer cell–intrinsic STING signaling primed by T cell–secreted cytokines, particularly IFN-γ, is required for enhanced *STING*^{KO} CAR-T cell fitness in combination with diABZI, highlighting the synergy between T cell–based immunotherapy and STING agonists.

Combination of STING^{KO} CAR-T Cells and diABZI Enhances Antitumor Efficacy, Remodels the Tumor Microenvironment, and Shows No Systemic Toxicity In Vivo

Based on our in vitro findings, we sought to translate our results in vivo. To directly apply our approach using human T cells, we utilized immunodeficient NOD-SCID-IL2R-gamma (NSG) mice, which permit human cell

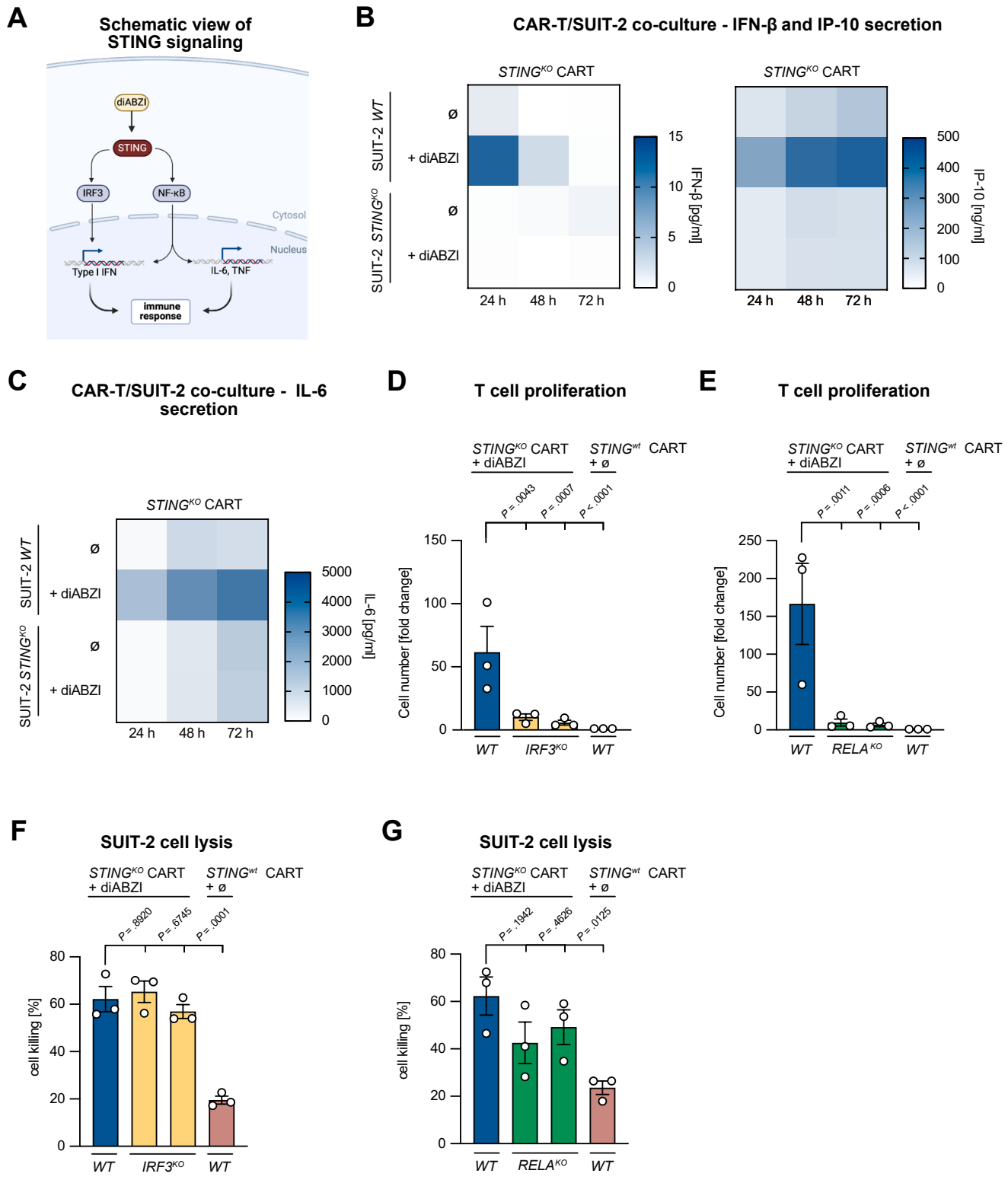

Figure 4. Tumor-intrinsic IRF3 and NF-κB support *STING*^{KO} CAR-T cell proliferation on STING agonist treatment. (*A*) Scheme of STING downstream pathways. Created with biorender.com. (*B* and *C*) A total of 0.2 $\times$ 10^6 *STING*^{KO} CAR-T cells were co-incubated with 0.2 $\times$ 10^6 of either *STING*^{wt} or *STING*^{KO} hMSLN-SUIT-2 cells for 72 hours in the presence or absence of diABZI. Protein levels of IFN-β, IP-10, and IL-6 in supernatants were determined by enzyme-linked immunosorbent assay at the indicated time points. Heat maps display mean concentrations of 3 independent experiments. (*D–G*) At day 14 of repetitive antigen stimulation, 6 $\times$ 10^3 CAR-T cells were co-incubated with 3 $\times$ 10^4 hMSLN-SUIT-2 cells. Graphs show mean $\pm$ SEM of 3 independent donors. (*D* and *E*) Absolute CAR-T cell counts were determined via flow cytometry. Fold changes were determined relative to *STING*^{wt} CAR-T cells + ø. Statistical analysis was conducted by 1-way analysis of variance (ANOVA) with Dunnett's multiple comparisons test on log-transformed data. (*F* and *G*) Cancer cell lysis after 72 hours was determined by LDH release assay. Statistical analysis was conducted by 1-way ANOVA with Dunnett's multiple comparisons test.

engraftment. Tumor cells were implanted SC, followed by IV injection of *STING*^{wt} or *STING*^{KO} human CAR-T cells or untransduced T cells. Mice received twice-weekly intratumoral injections of diABZI or vehicle control (Figure 6*A*). Although *STING*^{wt} CAR-T cells and untransduced T cells with diABZI moderately reduced tumor growth, *STING*^{KO} CAR-T cells plus diABZI exhibited the strongest tumor reduction (Figure 6*B*). Tumors explanted on day 28 revealed increased CD44 expression in both diABZI-treated CAR-T groups (Supplementary Figure 6*A*, left), but the CD44-to-LAG-3 ratio was highest in the *STING*^{KO} CAR-T plus diABZI condition (Supplementary Figure 6*A*, right). Pretreatment with diABZI before CAR-T injection resulted in increased intratumoral T cell numbers in this group (Supplementary Figure 6*B* and *C*). Mouse body weight remained stable across all groups (Supplementary Figure 6*D*).

Because xenograft models in immunodeficient mice do not capture the complex immune interactions of immunocompetent settings, and intratumoral injections have limited translational relevance, we developed a syngeneic model combining systemic (IV) diABZI administration with *STING*^{wt} or *STING*^{KO} murine CAR-T cells. We used KPC-derived T110299 PDAC cells transgenic for murine EpCAM (T11-EpCAM), and generated EpCAM-targeting murine CAR-T cells from WT or *Sting1*$^{-/-}$ mice. Tumor cells were implanted SC, followed by IV diABZI administration one day before CAR-T cell injection (Figure 6*C*). Mice then received twice-weekly systemic diABZI or vehicle injections for 3 additional times. Again, systemic diABZI reduced tumor volumes only in combination with *STING*^{KO} CAR-T cells (Figure 6*D*). Mice maintained stable body weight (Supplementary Figure 6*E*).

To investigate underlying mechanisms, we performed flow cytometry–based characterization of the TME (Supplementary Figure 7*A*). Intratumoral CAR-T cell numbers were highest in the *STING*^{KO} CAR-T plus diABZI group (Figure 6*E*). In addition, endogenous intratumoral CD4$^+$ and CD8$^+$ T cells upregulated CD69 in diABZI-treated mice, suggesting T cell activation beyond the transferred CAR-T population (Supplementary Figure 7*B*). Analysis of intratumoral myeloid cells revealed a reduction in tumor-associated macrophages (TAMs) in the combination group (Figure 6*F*), and remaining TAMs upregulated CD86, indicative of a more proinflammatory phenotype (Supplementary Figure 7*C*). Within the myeloid-derived suppressor cell (MDSC) compartment, monocytic MDSCs increased, while polymorphonuclear MDSC levels remained unchanged (Figure 6*F*). CD86 expression was unaltered in both subsets (Supplementary Figure 7*C*). We further examined immune activation in secondary-lymphoid organs. In tumor-draining lymph nodes and spleen, CD69 and CD86 were upregulated on endogenous T cells and D45$^+$CD3$^-$ immune cells, respectively (Supplementary Figure 7*D*), indicating that the combination therapy not only inflames the TME but also induces activation signals in lymphoid organs. To assess safety, we analyzed serum cytokines, clinical chemistry, and histopathology. Serum levels of proinflammatory cytokines (IFN-α, TNF, IL-6) were modestly elevated following diABZI administration but remained within tolerable limits (Figure 6*G*) without signs of cytokine release syndrome. CCL2, CCL4, CXCL9, and CXCL10 serum levels were also increased, while CCL3, IL-10, and granulocyte-macrophage colony-stimulating factor remained unchanged (Figure 6*G*, Supplementary Table 1). Liver and kidney function parameters and LDH remained stable (Supplementary Figure 7*E*). Histological evaluation of liver, kidney, lung, and spleen did not reveal any signs of tissue damage or inflammation (Supplementary Figure 8).

To further validate the therapeutic relevance of our findings in a more physiologic setting, we performed an orthotopic model by intrapancreatic injection of T11-EpCAM cells (Figure 6*H*). On termination, tumor weight was substantially reduced in the *STING*^{KO} CAR-T plus diABZI group (Figure 6*I*, left), and flow cytometry confirmed increased intratumoral CAR-T numbers (Figure 6*I*, right), indicating effective infiltration/persistence within the pancreatic TME.

Taken together, our data demonstrate that *STING*^{KO} CAR-T cells combined with diABZI enhance tumor control, increase CAR-T infiltration, and remodel the suppressive TME in immunodeficient and immunocompetent models. The combination was not associated with systemic toxicity, and its efficacy was preserved in a relevant orthotopic model that better recapitulates the anatomical features of human PDAC, supporting the translational potential of selectively uncoupling STING activation in T cells from the broader tumor and stromal compartments.

Discussion

In this study, we identified STING agonism to enhance CAR-T cell functionality in preclinical human and murine pancreatic cancer models. However, genetic ablation of *STING* in CAR-T cells was a critical prerequisite to protect them from detrimental outcomes of T cell–intrinsic STING signaling. Using a repetitive antigen stimulation model, *STING*^{KO} CAR-T cells, combined with the STING agonist diABZI, displayed superior anticancer functions. Mechanistically, cancer cell–intrinsic STING, IRF3, and NF-κB activation, as well as IFN-γ– and TNF-mediated STING priming, formed a synergistic feedback loop: CAR-T–derived cytokines primed cancer cell–intrinsic STING signaling, enhancing its agonist-induced activation and promoting CAR-T functionality. Moreover, this approach showed potent in vivo activity across xenograft and syngeneic models in vivo. These included an orthotopic PDAC model, confirming our findings in a physiologically relevant tumor environment.

Therapeutic STING agonism represents a promising concept to enhance antitumor immune responses. In our models, combination therapy enhanced CAR-T cell infiltration/persistence, reduced TAMs while promoting a shift toward a proinflammatory phenotype, and induced activation signals in antigen-presenting cells and T cells within tumor-draining lymph nodes. These findings align with prior reports suggesting that STING agonists can remodel the TME, activate inflammatory programs in cancer-

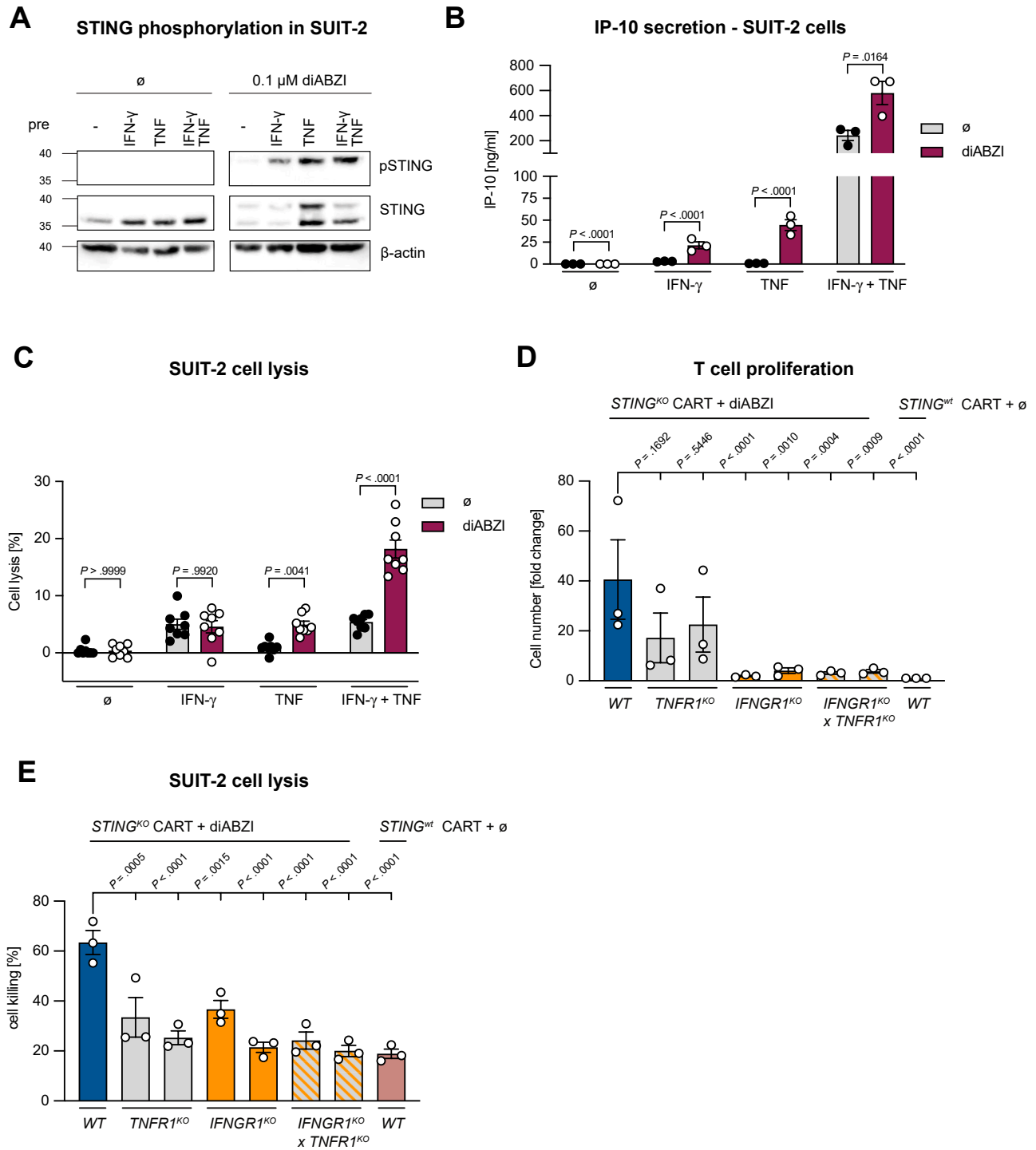

Figure 5. Priming of target cell–intrinsic STING activation by IFN-γ and TNF is crucial for enhanced *STING*^{KO} CAR-T cell fitness. (*A–C*) A total of 0.2 × 10^6 SUIT-2 cells were prestimulated for 2 hours with medium (−), 20 ng/mL IFN-γ, 20 ng/mL TNF, or the combination of both (IFN-γ/TNF). Subsequently, control medium or 0.1 μM diABZI was added for 22 hours. (*A*) Expression of STING and pSTING was determined by immunoblot. β-Actin was used as loading control. One representative blot of 3 independent experiments is shown. (*B*) IP-10 levels in supernatants were determined by enzyme-linked immunosorbent assay. Data show mean ± SEM of 3 independent experiments. Statistical analysis was conducted by 2-way analysis of variance (ANOVA) with Sidak's multiple comparisons test on log-transformed data. (*C*) Cell lysis was determined using LDH release assay. Graph shows mean ± SEM of 8 independent experiments. Statistical analysis was conducted by 2-way ANOVA with Sidak's multiple comparisons test. (*D* and *E*) At day 14 of repetitive antigen stimulation, 6 × 10^3 CAR-T cells were co-incubated with 3 × 10^4 hMSLN-SUIT-2 cells. Graphs show mean ± SEM of 3 independent donors. (*D*) Absolute CAR-T cell counts were determined via flow cytometry. Fold changes were determined relative to *STING*^{wt} CAR-T cells + ø. Statistical analysis was conducted by 1-way ANOVA with Dunnett's multiple comparisons test on log-transformed data. (*E*) Cancer cell lysis after 72 hours was determined by LDH release assay. Statistical analysis was conducted by one-way ANOVA with Dunnett's multiple comparisons test.

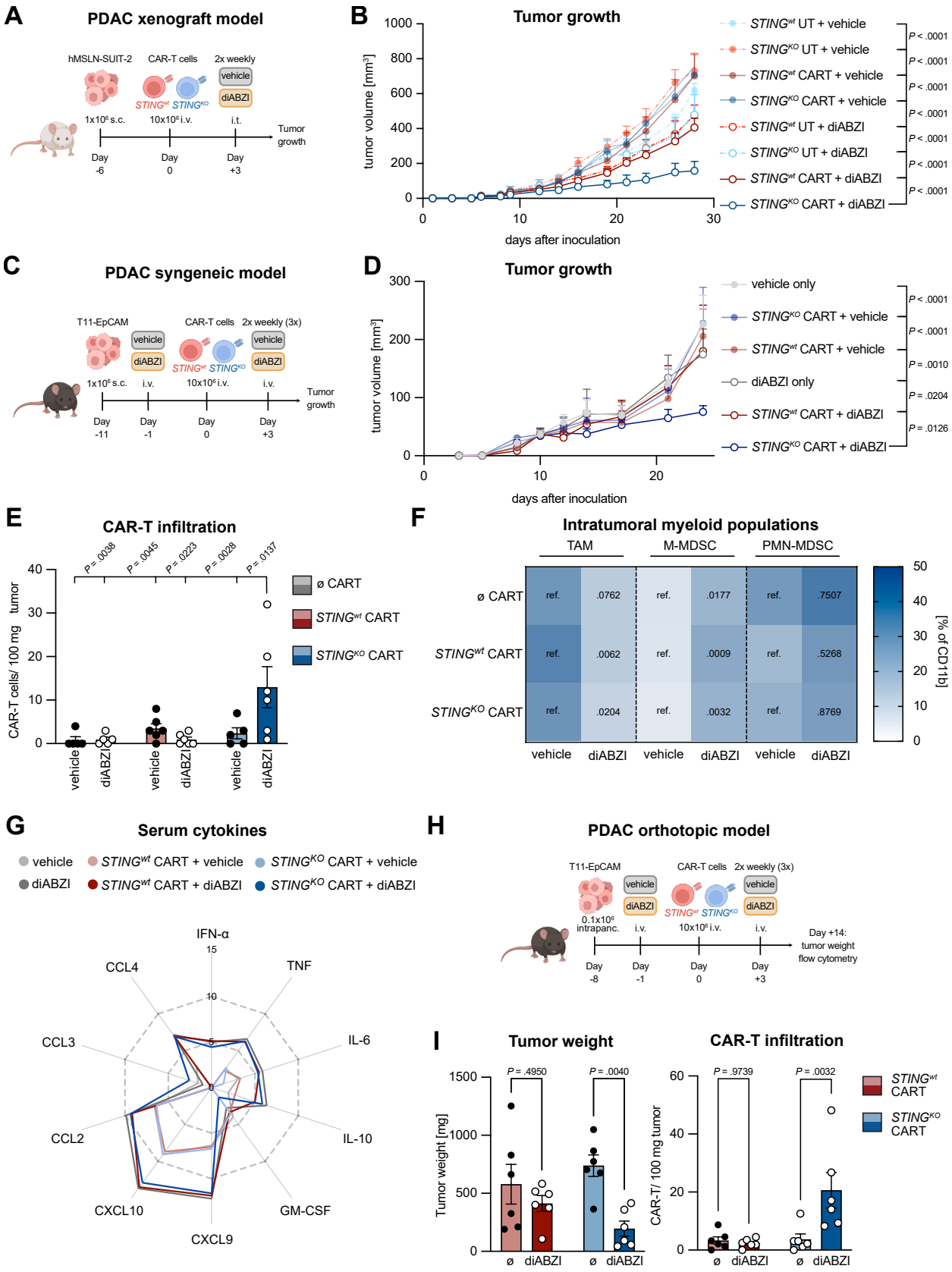
A
PDAC xenograft model
hMSLN-SUIT-2
CAR-T cells
2x weekly
vehicle
diABZI
STINGwt STINGKO
1x10⁶ s.c.
10x10⁶ i.v.
i.t.
Tumor growth
Day -6
Day 0
Day +3
B
Tumor growth
tumor volume [mm³]
days after inoculation
STINGwt UT + vehicle
STINGKO UT + vehicle
STINGwt CART + vehicle
STINGKO CART + vehicle
STINGwt UT + diABZI
STINGKO UT + diABZI
STINGwt CART + diABZI
STINGKO CART + diABZI
P < .0001
C
PDAC syngeneic model
T11-EpCAM
CAR-T cells
2x weekly (3x)
1x10⁶ s.c.
i.v.
10x10⁶ i.v.
Tumor growth
Day -11
Day -1
Day 0
Day +3
D
Tumor growth
tumor volume [mm³]
days after inoculation
vehicle only
STINGKO CART + vehicle
STINGwt CART + vehicle
diABZI only
STINGwt CART + diABZI
STINGKO CART + diABZI
P < .0001
P < .0001
P = .0010
P = .0204
P = .0126
E
CAR-T infiltration
CAR-T cells/ 100 mg tumor
P = .0038
P = .0045
P = .0223
P = .0028
P = .0137
ø CART
STINGwt CART
STINGKO CART
vehicle
diABZI
F
Intratumoral myeloid populations
TAM
M-MDSC
PMN-MDSC
ø CART
STINGwt CART
STINGKO CART
ref.
.0762
.0177
.7507
.0062
.0009
.5268
.0204
.0032
.8769
vehicle
diABZI
[% of CD11b]
G
Serum cytokines
vehicle
diABZI
STINGwt CART + vehicle
STINGwt CART + diABZI
STINGKO CART + vehicle
STINGKO CART + diABZI
IFN-α
TNF
IL-6
IL-10
GM-CSF
CXCL9
CXCL10
CCL2
CCL3
CCL4
H
PDAC orthotopic model
T11-EpCAM
CAR-T cells
2x weekly (3x)
0.1x10⁶ intrapanc.
i.v.
10x10⁶ i.v.
Day +14: tumor weight flow cytometry
Day -8
Day -1
Day 0
Day +3
I
Tumor weight
Tumor weight [mg]
P = .4950
P = .0040
ø
diABZI
CAR-T infiltration
CAR-T/ 100 mg tumor
P = .9739
P = .0032
STINGwt CART
STINGKO CART

associated fibroblasts, and stimulate endogenous antitumor immunity, also by inducing epitope spreading, thereby counteracting frequent cancer resistance mechanisms.[17,24,25] However, despite promising preclinical data, early clinical trials have not demonstrated sustained efficacy in solid cancers.[24,26] Although STING agonists effectively modulate the myeloid compartment, their limited in vivo pharmacokinetics and potential detrimental effects on particularly T cells, may restrict their efficacy.[27] Notably, STING activation in T cells induces antiproliferative programs and apoptosis.[12,28] To counteract this, we genetically deleted *STING* in CAR-T cells using CRISPR-Cas9, which has been established in adoptive T cell therapy to knock out inhibitory pathways in preclinical and early clinical studies without relevant off-target effects.[29] Thus, targeting T cell–intrinsic genes via CRISPR-Cas9 genome editing remains a safe and feasible strategy for clinical application.

A few reports have explored the combination of STING agonists and therapeutic T cells, mostly using cyclic-dinucleotide agonists or intratumoral application routes,[30–32] limiting the systemic applicability due to limited pharmacokinetics (degradation, cellular perturbation) and restricting its use in metastasized disease.[27,33,34] Here, we used the small molecule STING agonist diABZI designed for potent STING activation with increased membrane permeability and extended in vivo half-life, even when systemically administered.[18] This compound, currently under clinical investigation (NCT03843359), strongly induced T cell apoptosis unless T cells were protected by genomic *STING* knockout. *STING* deficiency was required to fully unleash the combinatorial potential of CAR-T cells and a small molecule agonist in vitro and in vivo. The local application and dosing of STING agonists in previous studies may have influenced outcomes, as therapeutic STING agonist dosing significantly impacts adaptive antitumor immunity.[35] Therefore, STING ablation in therapeutically administered T cells could enable stronger dosing regimens and systemic application routes.

Mechanistically, *STING*^{KO} CAR-T cells combined with diABZI showed increased proliferation, reduced exhaustion, expanded Tem populations, and decreased Teff. On diABZI treatment, cancer cells secreted IRF3- and NF-κB–dependent cytokines, which could be amplified by priming cancer cell–intrinsic STING signaling through T cell–derived factors. IFN-β and IL-6, proxies for IRF3 and NF-κB activation, are both linked to T cell regulation. Type-I interferons enhance T cell proliferation and upregulate antiapoptotic programs in T cell receptor–activated T cells, while inducing apoptosis in nonactivated T cells.[36] IL-6 promotes T cell survival and prevents activation-induced cell death, playing a key role in T cell biology.[37] Our findings suggest that enhanced CAR-T functionality result from the concerted action of multiple proinflammatory cytokines induced by STING-mediated IRF3 and NF-κB activation in cancer cells. Overall, our immunophenotypical analysis indicates that combining STING-deficient CAR-T cells with STING agonists could be a promising strategy to induce T cell–activating cytokines, leading to increased numbers of T cells with enhanced anticancer properties.[38,39]

Regarding target antigen selection, we employed mesothelin (MSLN) in the human system—a widely studied antigen in PDAC CAR-T trials.[40] Its expression is largely restricted to healthy mesothelial tissues, but is highly upregulated in malignancies such as pancreatic, ovarian, and lung cancer.[41] MSLN is considered a promising CAR target and is under clinical evaluation in multiple trials to assess safety and preliminary outcomes.[41] However, MSLN-targeting CAR-T cells have shown limited persistence and efficacy in solid tumors.[41] In the murine system, we used EpCAM as a target antigen based on the experiences in syngeneic models within our lab. Although biological differences between antigens, including density, shedding, spatial distribution, and susceptibility to antigen escape,[42] may influence CAR-T efficacy, the observed improvements in tumor control were consistent despite this antigen switch, supporting the robustness of our combination strategy. Importantly, our combination substantially improved tumor control in models highly resistant to CAR treatment alone, highlighting its potential for clinical translation. In addition, our approach exhibited a favorable safety profile, with no evidence of cytokine release syndrome (CRS) compared with preclinical CRS models or extrapolated to the human setting,[43,44] and no treatment-related organ toxicities based on clinical chemistry and histopathology. These data suggest that selective uncoupling of STING signaling in T cells, while maintaining its activity in other compartments, allows for safe and effective systemic application of STING agonists.

Figure 6. Combination of STING^{KO} CAR-T cells and diABZI enhances antitumor efficacy, remodels the TME, and shows no systemic toxicity in vivo. (*A*) Treatment scheme for xenograft CAR-T experiment. (*B*) Tumor growth is displayed. Graph shows mean ± SEM of pooled data from 2 independent experiments with n = 5–6 mice per CAR-T group and n = 3 mice per untransduced T group. Statistical analysis was performed using 2-way analysis of variance (ANOVA) with Dunnett's multiple comparisons test. *P* values for the last measurement are depicted. (*C*) Treatment scheme for syngeneic subcutaneous CAR-T experiment. (*D*) Tumor growth is displayed. Graph shows mean ± SEM of n = 5–6 mice per group. Statistical analysis was performed using 2-way ANOVA with Dunnett's multiple comparisons test. *P* values for the last measurement are depicted. (*E–G*) Tumors and blood sera were harvested 1 week after CAR-T injection. (*E*) Absolute counts of intratumoral CAR-T cells were determined using flow cytometry. Numbers per 100-mg tumor are shown as mean ± SEM of n = 5–6 mice per group. Statistical significance was calculated by 2-way ANOVA with Sidak's multiple comparisons test. (*F*) Heatmap displays mean frequencies of indicated populations among groups of n = 5–6 mice per group. Statistical significance was calculated by 2-way ANOVA with Sidak's multiple comparisons test. *P* values are indicated in the respective boxes. (*G*) Radar plot shows log2-transformed mean serum levels of indicated cytokines of n = 5–6 mice per group. (*H*) Treatment scheme for syngeneic orthotopic CAR-T experiment. (*I*) Tumors were harvested 2 weeks after CAR-T injection. Tumor weight was determined and absolute numbers of intratumoral CAR-T cells were analyzed using flow cytometry. Data are shown as mean ± SEM of n = 6 mice per group. Statistical significance was calculated by 2-way ANOVA with Sidak's multiple comparisons test.

Limitations

First, we utilized human cell line– and KPC-derived models, which may not fully recapitulate human PDAC heterogeneity and complexity. Second, although our approach demonstrated efficacy and safety, further evaluation in more advanced models such as patient-derived xenografts or humanized mouse systems would be desired to validate translatability. Last, long-term effects on CAR-T memory and potential immunopathology were not addressed and warrant future investigation in vivo.

Conclusions

In conclusion, our data propose that STING ablation in CAR-T cells is a promising strategy to harness the immunostimulatory potential of STING agonists. This combination improves CAR-T functionality and persistence and inflames the TME while preserving safety. These findings offer a compelling rationale for clinical exploration of $STING^{KO}$ CAR-T cells in combination with STING agonists for the treatment of poorly immunogenic solid tumors such as PDAC.

Declaration of Generative AI and AI-Assisted Technologies in the Writing Process

Portions of this manuscript were edited for clarity and conciseness using OpenAI's ChatGPT. The AI-assisted modifications were restricted to improving readability and conciseness, with all scientific content and conclusions remaining the sole responsibility of the authors.

Supplementary Material

Note: To access the supplementary material accompanying this article, visit the online version of *Gastroenterology* at www.gastrojournal.org, and at https://doi.org/10.1053/j.gastro.2026.01.031.

References

1. Siegel RL, Giaquinto AN, Jemal A. Cancer statistics, 2024. CA Cancer J Clin 2024;74:12–49.
2. Espinet E, Klein L, Puré E, et al. Mechanisms of PDAC subtype heterogeneity and therapy response. Trends Cancer 2022;8:1060–1071.
3. Sterner RC, Sterner RM. CAR-T cell therapy: current limitations and potential strategies. Blood Cancer J 2021;11:69.
4. Rafiq S, Hackett CS, Brentjens RJ. Engineering strategies to overcome the current roadblocks in CAR T cell therapy. Nat Rev Clin Oncol 2020;17:147–167.
5. Young RM, Engel NW, Uslu U, et al. Next-generation CAR T-cell therapies. Cancer Discov 2022;12:1625–1633.
6. Woo SR, Fuertes MB, Corrales L, et al. STING-dependent cytosolic DNA sensing mediates innate immune recognition of immunogenic tumors. Immunity 2014;41:830–842.
7. Zhu Y, An X, Zhang X, et al. STING: a master regulator in the cancer-immunity cycle. Mol Cancer 2019;18:152.
8. Jing W, McAllister D, Vonderhaar EP, et al. STING agonist inflames the pancreatic cancer immune microenvironment and reduces tumor burden in mouse models. J Immunother Cancer 2019;7:115.
9. Vonderhaar EP, Barnekow NS, McAllister D, et al. STING activated tumor-intrinsic type I interferon signaling promotes CXCR3 dependent antitumor immunity in pancreatic cancer. Cell Mol Gastroenterol Hepatol 2021;12:41–58.
10. Ager CR, Boda A, Rajapakshe K, et al. High potency STING agonists engage unique myeloid pathways to reverse pancreatic cancer immune privilege. J Immunother Cancer 2021;9:e003246.
11. Wu J, Chen Y-J, Dobbs N, et al. STING-mediated disruption of calcium homeostasis chronically activates ER stress and primes T cell death. J Exp Med 2019;216:867–883.
12. Kuhl N, Linder A, Philipp N, et al. STING agonism turns human T cells into interferon-producing cells but impedes their functionality. EMBO Rep 2023;24:e55536.
13. Linder A, Bauernfried S, Cheng Y, et al. CARD8 inflammasome activation triggers pyroptosis in human T cells. EMBO J 2020;39:e105071.
14. Cadilha BL, Benmebarek MR, Dorman K, et al. Combined tumor-directed recruitment and protection from immune suppression enable CAR T cell efficacy in solid tumors. Sci Adv 2021;7:eabi5781.
15. Lesch S, Blumenberg V, Stoiber S, et al. T cells armed with C-X-C chemokine receptor type 6 enhance adoptive cell therapy for pancreatic tumours. Nat Biomed Eng 2021;5:1246–1260.
16. Bankhead P, Loughrey MB, Fernández JA, et al. QuPath: open source software for digital pathology image analysis. Sci Rep 2017;7:16878.
17. Kabashima A, Matsuo Y, Ito S, et al. cGAS-STING signaling encourages immune cell overcoming of fibroblast barricades in pancreatic cancer. Sci Rep 2022;12:10466.
18. Ramanjulu JM, Pesiridis GS, Yang J, et al. Design of amidobenzimidazole STING receptor agonists with systemic activity. Nature 2018;564:439–443.
19. Argani P, Iacobuzio-Donahue C, Ryu B, et al. Mesothelin is overexpressed in the vast majority of ductal adenocarcinomas of the pancreas: identification of a new pancreatic cancer marker by serial analysis of gene expression (SAGE)1. Clin Cancer Res 2001;7:3862–3868.
20. Hopfner KP, Hornung V. Molecular mechanisms and cellular functions of cGAS-STING signalling. Nat Rev Mol Cell Biol 2020;21:501–521.
21. Benmebarek M-R, Karches CH, Cadilha BL, et al. Killing mechanisms of chimeric antigen receptor (CAR) T Cells. Int J Mol Sci 2019;20:1283.
22. Xiong H, Xi Y, Yuan Z, et al. IFN-γ activates the tumor cell-intrinsic STING pathway through the induction of

DNA damage and cytosolic dsDNA formation. Oncoimmunology 2022;11:2044103.
23. Zhang L, Wei X, Wang Z, et al. NF-κB activation enhances STING signaling by altering microtubule-mediated STING trafficking. Cell Rep 2023;42:112185.
24. Hines JB, Kacew AJ, Sweis RF. The development of STING agonists and emerging results as a cancer immunotherapy. Curr Oncol Rep 2023;25:189–199.
25. Conde E, Vercher E, Soria-Castellano M, et al. Epitope spreading driven by the joint action of CART cells and pharmacological STING stimulation counteracts tumor escape via antigen-loss variants. J Immunother Cancer 2021;9:e003351.
26. Le Naour J, Zitvogel L, Galluzzi L, et al. Trial watch: STING agonists in cancer therapy. Oncoimmunology 2020;9:1777624.
27. Amouzegar A, Chelvanambi M, Filderman JN, et al. STING agonists as cancer therapeutics. Cancers 2021; 13:2695.
28. Gulen MF, Koch U, Haag SM, et al. Signalling strength determines proapoptotic functions of STING. Nat Commun 2017;8:427.
29. Dimitri A, Herbst F, Fraietta JA. Engineering the next-generation of CAR T-cells with CRISPR-Cas9 gene editing. Mol Cancer 2022;21:78.
30. Xu N, Palmer DC, Robeson AC, et al. STING agonist promotes CAR T cell trafficking and persistence in breast cancer. J Exp Med 2021;218:e20200844.
31. Smith TT, Moffett HF, Stephan SB, et al. Biopolymers codelivering engineered T cells and STING agonists can eliminate heterogeneous tumors. J Clin Invest 2017; 127:2176–2191.
32. Uslu U, Sun L, Castelli S, et al. The STING agonist IMSA101 enhances chimeric antigen receptor T cell function by inducing IL-18 secretion. Nat Commun 2024;15:3933.
33. Su M, Zheng J, Gan L, et al. Second messenger 2'3'-cyclic GMP-AMP (2'3'-cGAMP): synthesis, transmission, and degradation. Biochem Pharmacol 2022;198:114934.
34. Moser JC, Alistar A, Cohen E, et al. 618 Phase 1 clinical trial evaluating the safety, biologic and anti-tumor activity of the novel STING agonist IMSA101 administered both as monotherapy and in combination with PD-(L)1 checkpoint inhibitors. J Immunother Cancer 2023;11:A704.
35. Sivick KE, Desbien AL, Glickman LH, et al. Magnitude of therapeutic STING activation determines $CD8^+$ T cell-mediated anti-tumor immunity. Cell Rep 2018; 25:3074–3085.e5.
36. Crouse J, Kalinke U, Oxenius A. Regulation of antiviral T cell responses by type I interferons. Nat Rev Immunol 2015;15:231–242.
37. Li B, Jones LL, Geiger TL. IL-6 promotes T cell proliferation and expansion under inflammatory conditions in association with low-level RORγt expression. J Immunol 2018;201:2934–2946.
38. Anderson AC, Joller N, Kuchroo VK. Lag-3, Tim-3, and TIGIT: co-inhibitory receptors with specialized functions in immune regulation. Immunity 2016;44:989–1004.
39. Fraietta JA, Lacey SF, Orlando EJ, et al. Determinants of response and resistance to CD19 chimeric antigen receptor (CAR) T cell therapy of chronic lymphocytic leukemia. Nat Med 2018;24:563–571.
40. Czaplicka A, Lachota M, Paczek L, et al. Chimeric antigen receptor T cell therapy for pancreatic cancer: a review of current evidence. Cells 2024;13:101.
41. Klampatsa A, Dimou V, Albelda SM. Mesothelin-targeted CAR-T cell therapy for solid tumors. Exp Opin Biol Ther 2021;21:473–486.
42. Nasiri F, Safarzadeh Kozani P, Salem F, et al. Mechanisms of antigen-dependent resistance to chimeric antigen receptor (CAR)-T cell therapies. Cancer Cell Int 2025;25:64.
43. Giavridis T, van der Stegen SJC, Eyquem J, et al. CAR T cell-induced cytokine release syndrome is mediated by macrophages and abated by IL-1 blockade. Nat Med 2018;24:731–738.
44. Norelli M, Camisa B, Barbiera G, et al. Monocyte-derived IL-1 and IL-6 are differentially required for cytokine-release syndrome and neurotoxicity due to CAR T cells. Nat Med 2018;24:739–748.

Received March 1, 2025. Accepted January 23, 2026.

Correspondence
Address correspondence to: Veit Hornung, MD, Gene Center and Department of Biochemistry, Ludwig-Maximilians-Universität München, Feodor-Lynen-Strasse 25, 81377 Munich, Germany. e-mail: veit.hornung@lmu.de.

Acknowledgments
We want to thank Zeynep Ünal (Department of Pediatrics, LMU University Hospital) and Luana Messa and Vanessa Wittmann (all Institute of Clinical Pharmacology, LMU University Hospital) for technical assistance in mouse experiments and Maria del Socorro Escobar Lopez (Department of Medicine II, LMU University Hospital) for culturing AsPC-1 cells. We kindly thank Claudia Ludwig and Jochen Rech for technical support in isolation of primary immune cells and CRISPR-Cas9 knockout generation (all Gene Center, LMU Munich) and Britta Pauli for technical assistance in mouse serum analysis (Institute of Laboratory Medicine, LMU University Hospital).

CRediT Authorship Contributions
Ignazio Piseddu, MD (Conceptualization: Equal; Data curation: Supporting; Formal analysis: Equal; Funding acquisition: Supporting; Investigation: Lead; Methodology: Lead; Resources: Supporting; Visualization: Lead; Writing – original draft: Lead; Writing– review & editing: Lead)
Rebekka Endres (Investigation: Equal; Methodology: Equal; Visualization: Equal; Writing – review & editing: Equal)
Fabian Lanzl (Investigation: Equal; Methodology: Equal; Visualization: Equal; Writing – review & editing: Equal)
Linda Hammann, MSc (Investigation: Supporting; Methodology: Supporting; Writing review & editing: Equal)
Marleen Bérouti, PhD (Investigation: Supporting; Methodology: Supporting; Writing review & editing: Equal)
Matthias Thaler, MD (Investigation: Supporting; Methodology: Supporting; Writing review & editing: Equal)
Lisa Fahr, PhD (Investigation: Supporting; Methodology: Supporting; Writing – review & editing: Equal)
Hannah Fischer, PhD (Investigation: Supporting; Methodology: Supporting; Writing review & editing: Equal)
Varvara Varlamova, MSc (Investigation: Supporting; Methodology: Supporting; Writing – review & editing: Equal)
Jan Gärtig, PhD (Investigation: Supporting; Methodology: Supporting; Writing review & editing: Equal)
Daniel Nixdorf, PhD (Investigation: Supporting; Methodology: Supporting; Writing review & editing: Equal)
Patrick Layritz (Investigation: Supporting; Methodology: Supporting; Writing review & editing: Equal)
Charlotte Marx, PhD (Investigation: Supporting; Methodology: Supporting; Writing review & editing: Equal)
Christine Hörth (Investigation: Supporting; Methodology: Supporting; Writing review & editing: Equal)
Catharina Witte (Investigation: Supporting; Methodology: Supporting; Writing – review & editing: Equal)
Alpay Bulut (Investigation: Supporting; Methodology: Supporting; Writing review & editing: Equal)

David Illig, PhD (Investigation: Supporting; Methodology: Supporting; Writing – review & editing: Equal)
Anne Marie Senz, PhD (Methodology: Supporting; Writing – review & editing: Equal)
Lesca Holdt, MD (Investigation: Supporting; Methodology: Supporting; Writing review & editing: Equal)
Ivonne Regel, PhD (Investigation: Supporting; Methodology: Supporting; Writing review & editing: Equal)
Adrian Gottschlich, MD (Investigation: Supporting; Methodology: Supporting; Writing review & editing: Equal)
Marion Subklewe, MD (Supervision: Supporting; Writing – review & editing: Equal)
Julia Mayerle, MD (Conceptualization: Supporting; Funding acquisition: Supporting; Supervision: Equal; Writing – review & editing: Equal)
David Anz, MD (Resources: Supporting; Supervision: Supporting; Writing – review & editing: Equal)
Sebastian Kobold, MD (Resources: Equal; Supervision: Equal; Writing – review & editing: Equal)
Andreas Linder, MD (Conceptualization: Supporting; Methodology: Supporting; Supervision: Supporting; Writing – review & editing: Supporting)
Veit Hornung, MD (Conceptualization: Lead; Formal analysis: Equal; Funding acquisition: Lead; Project administration: Lead; Resources: Lead; Supervision: Lead; Validation: Lead; Writing – original draft: Lead; Writing – review & editing: Lead)

Conflicts of interest

These authors disclose the following: Ignazio Piseddu reports reimbursement of travel expenses and lecture honoraria from Roche and received lecture honoraria from Falk Foundation and third-party funding for scientific research from Novartis. Adrian Gottschlich received research support from Tabby Therapeutics and from Nanogami for work unrelated to the paper. Marion Subklewe has received research funding from Amgen, BMS/Celgene, Gilead/Kite, Janssen, Miltenyi Biotech, Molecular Partners, Novartis, Roche, Seagen, and Takeda; honoraria from AbbVie, Amgen, AvenCell, BMS, CanCell Therapeutics, Gilead, Janssen, Miltenyi Biomedicine, Molecular Partners, Pfizer, and Roche; and was invited as speaker by AstraZeneca, BMS, Gilead/Kite, GSK, Janssen, LAWG, Novartis, Pfizer, Roche, and Springer Healthcare. Sebastian Kobold has received honoraria from Cymab, Plectonic, TCR2 Inc., Miltenyi, Galapagos, Novartis, BMS, and GSK. Sebastian Kobold is an inventor of several patents in the field of immuno-oncology. Sebastian Kobold received license fees from TCR2 Inc and Carina Biotech and received research support from TCR2 Inc, Tabby Therapeutics, Catalym GmBH, Plectonic GmBH, and Arcus Bioscience for work unrelated to the manuscript. The remaining authors disclose no conflicts.

Funding

This work was supported by grants from the Bavarian Cancer Research Center (BZKF) (to Ignazio Piseddu), the *Stiftungen zu Gunsten der Medizinischen Fakultät* (Cluster 1, to Ignazio Piseddu), the Novartis Foundation (InCa prize awarded to Ignazio Piseddu), the ERC (ERC-2020-ADG–101018672 ENGINES, to Veit Hornung), and the Deutsche Forschungsgemeinschaft (German Research Foundation, SFB TRR 338 project-ID: 452881907 and SFB TRR 237 project-ID: 369799452, to Veit Hornung). This study was further supported by the Förderprogramm für Forschung und Lehre der Medizinischen Fakultät der LMU (grant number 1138 to Adrian Gottschlich), the BZKF (Adrian Gottschlich and TANGO to Sebastian Kobold), the DFG (grant number GO 3823/1–1 to Adrian Gottschlich; grant numbers KO5055–2–1 and KO5055/3–1 to Sebastian Kobold; grant number NI 2469/1–1 to Daniel Nixdorf), the international doctoral program "i-Target: immunotargeting of cancer" (funded by the Elite Network of Bavaria; to Sebastian Kobold), the Melanoma Research Alliance (grant number 409510 to Sebastian Kobold), Marie Sklodowska-Curie Training Network for Optimizing Adoptive T Cell Therapy of Cancer (funded by the Horizon 2020 program of the European Union; grant 955575 to Sebastian Kobold), Marie Sklodowska-Curie Training Network for Tracking and Controlling Therapeutic Immune Cells in Cancer (funded by the Horizon program of the European Union; grant 101168810 to Sebastian Kobold), Else Kröner-Fresenius-Stiftung (to Adrian Gottschlich, 2025_EKEA-16 to Ignazio Piseddu, and IOLIN to Sebastian Kobold), German Cancer Aid (AvantCAR.de and grant number 70117182 to Sebastian Kobold, grant number 70115514 to Adrian Gottschlich), Ernst Jung Stiftung (to Sebastian Kobold), Institutional Strategy LMUexcellent of LMU Munich (within the framework of the German Excellence Initiative; to Sebastian Kobold), the Go-Bio-Initiative (to Sebastian Kobold), the m4-Award of the Bavarian Ministry for Economical Affairs (to Sebastian Kobold), Bundesministerium für Bildung und Forschung (to Sebastian Kobold), European Research Council (StG 756017, PoC 101100460, and CoG 101124203 to Sebastian Kobold), by the SFB TRR 338 project-ID: 452881907 (to Sebastian Kobold), Fritz-Bender Foundation (to Sebastian Kobold), Deutsche José Carreras Leukämie Stiftung (to Sebastian Kobold), Hector Foundation (to Sebastian Kobold), Bavarian Research Foundation (BAYCELLATOR to Sebastian Kobold), the Bruno and Helene Jöster Foundation (360° CAR to Sebastian Kobold), the Monika Kutzner Foundation (to Sebastian Kobold), the Rurainski Foundation (to Sebastian Kobold), the Brigitte and Dr Konstanze Wegener Foundation (to Sebastian Kobold), and the DKTK School of Oncology (to Adrian Gottschlich and Sebastian Kobold). David Anz was supported by the German Research Foundation (SFB TRR 355 project-ID: 490846870).

Data Availability

All data are available on request from the corresponding author.